Journal of Alloys and Compounds 509 (2011) 7427–7433

Contents lists available at ScienceDirect

Journal of Alloys and Compounds

journal homepage: www.elsevier.com/locate/jallcom

Structural and optical investigations on Dy^{3+} doped boro-tellurite glasses

K. Maheshvaran, K. Marimuthu*

Department of Physics, Gandhigram Rural University, Gandhigram 624 302, India

ARTICLE INFO

Article history:
Received 2 November 2010
Received in revised form 7 April 2011
Accepted 8 April 2011
Available online 16 April 2011

PACS:
78.30Ly
78.40Pg
78.47Cd
78.55Qr

Keywords:
Amorphous materials
Oxide materials
Optical properties
Luminescence
X-ray diffraction

ABSTRACT

Dy^{3+} doped boro-tellurite glasses were prepared by following melt quenching technique with the chemical composition $(69-x)H_3BO_3 + xTeO_2 + 15Mg_2CO_3 + 15K_2CO_3 + 1Dy_2O_3$ (where $x = 0, 10, 20, 30$ and 40 wt%) by varying the tellurium dioxide content. The structural and optical properties have been studied through XRD, FTIR, absorption, luminescence and decay time measurements. The XRD pattern has been used to confirm the amorphous nature of the prepared glasses. The FTIR spectra reveals the presence of B–O vibrations and Te–O stretching modes of TeO_3 and TeO_6 units in the prepared glasses. The UV–vis–NIR absorption spectra were used to calculate the oscillator strength, bonding parameters ($\bar{\beta}$ and δ) and Judd–Ofelt intensity parameters (Ω_λ, $\lambda = 2$, 4 and 6). The radiative transition probability (A), stimulated emission cross section (σ_P^E) and the experimental, calculated branching ratios (β_R) have been calculated from the luminescence spectra corresponding to $^4F_{9/2} \rightarrow {}^6H_{11/2}$, $^6H_{13/2}$, and $^6H_{15/2}$ excited state transitions. The structural and optical properties corresponding to the compositional changes were discussed and compared with the similar studies.

1. Introduction

Tellurite based glass is an excellent linear and non-linear optical material due to its peculiar properties like low melting temperature, high dielectric constant, high refractive index, large third order non linear susceptibility and good infrared transmissivity [1,2]. Recently, the study on rare earth doped materials gained significant importance due to their potential applications in the field of photonics as optical data storage, display monitors, X-ray imaging, sensors, lasers, up-conversion and amplifiers for fiber optic communications [3]. Studies on the optical properties of the rare earth ions in glasses provide fundamental data that includes transition position and cross section, transition probabilities, radiative and non radiative decay rates, branching ratio, etc., for the excited states. This data is essential to design optical devices such as laser, color displays, up converters and fiber amplifiers. In order to identify new optical devices for specific utility or devices with enhanced performance active work is being carried out by selecting appropriate new hosts doped with rare earth ions [4].

There are two types of structural units namely trigonal bipyramid (tbp) and trigonal pyramid (tp) TeO_2 which are responsible for the attractive properties arising from these tellurite based glasses. In the tbp unit, a lone pair of electron occupies one of the equatorial sites of tellurium sp^3d hybrid orbitals and oxygen atoms occupy the other two equatorial and axial sites. When alkali oxides are added to tellurium oxide, the concentration of the tp units in which a lone pair of electron occupies one of the tellurium sp^3 hybrid orbital is increased [1,5]. Ardelean et al. [6] studied the structural and magnetic properties of boro-tellurite glasses. Tellurite glasses combine the attributes of wide transmission (0.35–6 μm), good glass stability, rare earth ion solubility, slow corrosion rate. Lowest phonon energy spectrum arising from oxide glass formers and high non linear refractive index have been already reported by Wang et al. [7].

The present work reports the structural and optical behavior of Dy^{3+} doped boro-tellurite glasses. The structure of the Dy^{3+} doped glasses has been studied through XRD and FTIR spectra. The optical behavior of the glasses has been studied through absorption, photoluminescence and lifetime measurements. The radiative parameters for the excited states of Dy^{3+} ions were calculated following the Judd–Ofelt theory. Decay time measurements have also been studied and these results were compared with the similar Dy^{3+} glasses.

2. Experimental

In the present study Dy^{3+} doped boro-tellurite glasses have been prepared by following conventional melt quenching technique [8]. The starting materials H_3BO_3, TeO_2, Mg_2CO_3, K_2CO_3 and Dy_2O_3 used in the study were of analytical grade (99.99%

* Corresponding author. Tel.: +91 451 2452371; fax: +91 451 2454466.
E-mail address: mari_ram2000@yahoo.com (K. Marimuthu).

0925-8388/$ – see front matter © 2011 Elsevier B.V. All rights reserved.
doi:10.1016/j.jallcom.2011.04.055

Table 1
Physical properties of the Dy^{3+} doped boro-tellurite glasses.

S. No.	Physical properties	B0TD	B1TD	B2TD	B3TD	B4TD
1	Density, ρ (g/cm^3)	3.14	3.46	4.32	4.63	5.83
2	Refractive index, n_d (589.3 nm)	1.596	1.624	1.656	1.682	1.704
3	Rare earth ion concentration, N ($\times 10^{20}$ ions/cm^3)	4.535	4.472	5.054	4.947	5.731
4	Polaron radius, r_p (Å)	5.2444	5.268	5.058	5.094	4.850
5	Inter ionic distance, r_i (Å)	13.015	13.076	12.553	12.643	12.038
6	Field strength, F (10^{14} cm^{-2})	1.770	1.754	1.903	1.876	2.070
7	Electronic polarizability, α_e (10^{-22} cm^3)	1.792	1.885	1.736	1.828	1.617
8	Molar refractivity, R_m (cm^3)	8.217	6.481	6.736	6.148	5.098
9	Dielectric constant (ε)	2.547	2.637	2.742	2.829	2.903
10	Reflection losses, R (%)	5.271	5.655	6.100	6.466	6.778

purity). The batch composition (in wt%) of the Dy^{3+} doped boro-tellurite glasses are as follows:

$69B_2O_3 + 0TeO_2 + 15MgO + 15K_2O + 1Dy_2O_3$ B0TD

$59B_2O_3 + 10TeO_2 + 15MgO + 15K_2O + 1Dy_2O_3$ B1TD

$49B_2O_3 + 20TeO_2 + 15MgO + 15K_2O + 1Dy_2O_3$ B2TD

$39B_2O_3 + 30TeO_2 + 15MgO + 15K_2O + 1Dy_2O_3$ B3TD

$29B_2O_3 + 40TeO_2 + 15MgO + 15K_2O + 1Dy_2O_3$ B4TD

About 7 g of the batches of composition were taken in an agate mortar and ground thoroughly to obtain homogeneous mixture. The mixture was then taken in to a porcelain crucible and heated to 900 °C in an electrical furnace for 45 min. The melt was then quickly poured onto a preheated brass plate and pressed with another brass plate to obtain circular shaped glass samples of thickness about 1.5 mm. The glass samples were annealed at 350 °C for 7 h to avoid the formation of cracks, air bubbles and to enhance the mechanical strength. The glasses were polished to obtain planar faces before to take optical measurements.

The X-ray diffraction measurements were carried out using JEOL 8530 X-ray diffractometer employing CuKα radiation. The infrared spectra of the glass samples were recorded using Perkin-Elmer paragon 500 FTIR spectrometer with a resolution of 4 cm^{-1} in the wavenumber range 400-4000 cm^{-1}. The optical absorption measurements were made using CARY 500 spectrometer in the wave length range 360–2000 nm with a resolution of ±0.1 nm. The photoluminescence measurements were made using Perkin-Elmer LS55 spectrometer in the wavelength range 450–700 nm with a resolution of ±1.0 nm. The decay luminescence measurements were measured through a digital storage oscilloscope (Tektronix TDS1001B) interfaced to a personal computer that records and averages the signal.

The glass density was measured following the Archimedes principle using xylene as an immersion liquid and the refractive index of the prepared glasses were measured using Abbe refractrometer at sodium wavelength. The measured physical properties of the Dy^{3+} doped boro-tellurite glasses are presented in Table 1.

3. Results and discussion

3.1. XRD and FTIR analysis

X-ray diffraction pattern of the boro-tellurite glasses recorded in the range of $5^\circ \le \theta \le 80^\circ$ exhibits broad diffuse scattering at lower angles suggesting the lower range structural disorder which confirms the amorphous nature of the prepared glasses. XRD pattern of the Dy^{3+}:B0TD glass is shown in Fig. 1.

The infrared transmittance spectra of the Dy^{3+} doped boro-tellurite glasses recorded between 400 and 4000 cm^{-1} are shown in Fig. 2. The peak frequencies and their assignments are presented in Table 2. The observed band position around 3557 cm^{-1} can be attributed to the fundamental stretching of hydroxyl groups [9–11]. The band position around 2925 cm^{-1} is assigned to the hydrogen bond. The band around 1640 cm^{-1} reveals the stretching vibration of borate triangles. The broad band around 1430 cm^{-1} attribute the asymmetric mode of B–O stretching vibrations in BO_3 unit from boroxol rings [12]. The band at 1240 cm^{-1} has been ascribed to the B–O stretching vibration of BO_3 units in boroxol rings. The absorption band at 1090 cm^{-1} is assigned to B–O stretching vibration of BO_4 units in triborate, tetraborate and pentaborate groups and

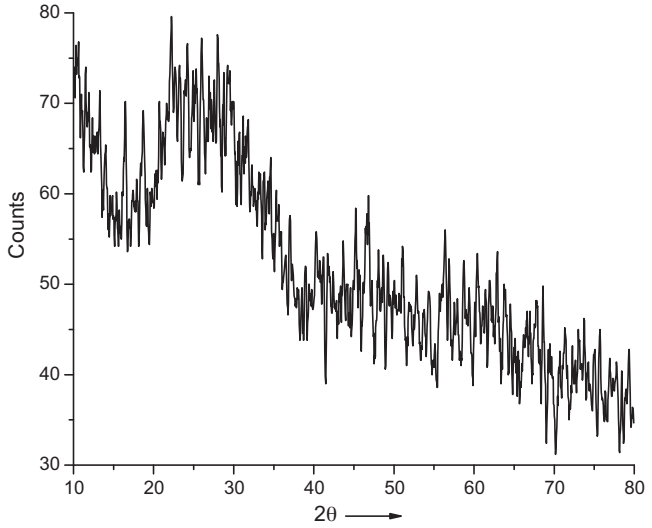

Fig. 1. XRD Pattern of the Dy^{3+}:B0TD glass.

the band centered around 1020 cm^{-1} is due to the B–O vibrations attached with the BO_4 units. The band centered around 839 cm^{-1} attributes to the Te–O bending vibration in TeO_3 units [9,12]. The peaks around 710 cm^{-1} attribute to the Te–O stretching mode of [TeO_3] and [TeO_6] units. The band position around 440 cm^{-1} is attributed to the Te–O–Te or O–Te–O linkages of the bending vibrations [9,12,13]. It is observed that the band positions around 839 and 440 cm^{-1} appear when the tellurium di-oxide content increases.

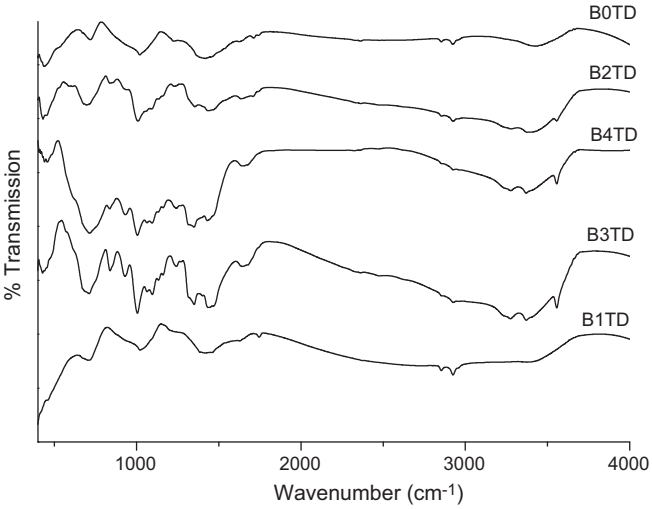

Fig. 2. Infrared spectra of Dy^{3+} doped boro-tellurite glasses.

Table 2
Peak table of FTIR spectra (in cm^{-1}) of Dy^{3+} doped boro-tellurite glasses.

S. No.	B0TD	B1TD	B2TD	B3TD	B3TD	Assignments
1	3436	3430	3557	3556	3556	Fundamental stretching of OH groups
2	2925	2924	2925	2924	2924	Hydrogen bonding
3	1626	1630	1634	1643	1648	Stretching vibration of borate triangles
4	1417	1421	1434	1446	1430	B–O^- vibrations
5	1228	–	1228	1242	1242	Stable tetrahedral BO_4 units
6	–	1084	1090	1095	1094	BO_4 stretching in the tri, tetra and pentaborate group
7	1020	1022	1008	1004	1004	B–O vibrations attached with BO_4 units
8	–	–	839	839	836	Te–O bending vibration in TeO_3 units
9	–	710	697	712	716	Te–O stretching mode of TeO_3 and TeO_6
10	–	–	431	428	439	Te–O–Te or O–Te–O linkage bending vibrations

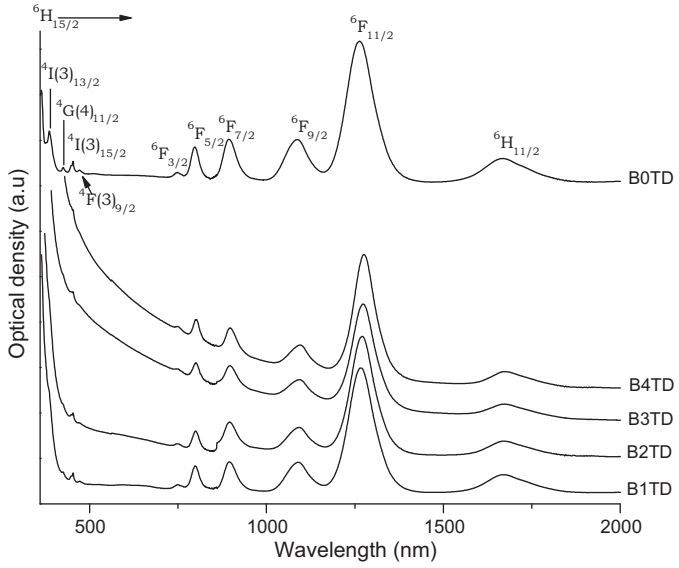

Fig. 3. Absorption spectra of the Dy^{3+} doped boro-tellurite glasses.

3.2. Absorption spectra

The room temperature absorption spectra of Dy^{3+} doped boro-tellurite glasses are recorded in the wavelength range 360–2000 nm and are shown in Fig. 3. The spectra consist of 10 transitions originating from the $^6H_{15/2}$ ground state similar to other absorption spectra of Dy^{3+} doped glasses [14–16]. The absorption bands arise from the $^6H_{11/2}$, $^6F_{11/2}$, $^6F_{9/2}$, $^6F_{7/2}$, $^6F_{5/2}$, $^6F_{3/2}$, $^4F(3)_{9/2}$, $^4I(3)_{15/2}$, $^4G(4)_{11/2}$ and $^4I(3)_{13/2}$ states of Dy^{3+} ions. The $^6F_{5/2} \rightarrow {}^6H_{11/2}$ transition located at around 7820 cm^{-1} is a hypersensitive transition satisfies the selection rule $|\Delta S| = 0$, $|\Delta L| \leq 2$, $|\Delta J| \leq 2$ [17]. The band positions (in cm^{-1}) and their assignments for all the prepared glasses are presented in Table 3.

Dy^{3+}–ligand bonding parameters ($\bar{\beta}$, δ) have been calculated from the Nephelauxetic ratio (β) using the below given relation [18]

$$\beta = \frac{\nu_c}{\nu_a} \quad (1)$$

where ν_c is the wave number (in cm^{-1})of a particular transition for the rare earth ion under investigation and ν_a is the wave number (in cm^{-1}) for the same transition of an aqua-ion. From the average values of β (referred as $\bar{\beta}$) the bonding parameter is calculated using the formula [18]

$$\delta = \frac{1 - \bar{\beta}}{\bar{\beta}} \times 100 \quad (2)$$

The bonding will be covalent/ionic depending on the positive or negative sign of δ. The bonding parameters ($\bar{\beta}$, δ) for the prepared Dy^{3+}:boro-tellurite glasses have been presented in Table 3 and it is observed from the table that the prepared glasses posses ionic nature and the ionic nature gradually increases when the tellurium di-oxide content increases in the host matrix.

3.3. Oscillator strengths and Judd–Ofelt analysis

The measurement of intensities of the optical absorption bands of RE^{3+} ions plays a major role in understanding their optical properties [19,20]. The oscillator strengths (f_{exp}) of the absorption bands are determined experimentally using the following formula [21]

$$f_{exp} = 4.318 \times 10^{-9} \int \varepsilon(\nu) d\nu \quad (3)$$

where $\varepsilon(\nu)$ is the molar extinction coefficient at a wave number ν cm^{-1}. The experimental oscillator strengths (f_{exp}) of the Dy^{3+}:BXTD glasses were evaluated by measuring the integrated areas of the observed absorption transitions and are used in the frame work of Judd–Ofelt (JO) theory [22,23]. The transition intensities are characterized by the JO intensity parameters Ω_λ ($\lambda = 2$, 4 and 6) which depend on the local environment of the rare earth ion. The calcu-

Table 3
Observed band positions (cm^{-1}) and bonding parameters ($\bar{\beta}$ and δ) of Dy^{3+} doped boro-tellurite glasses.

Transition	B0TD	B1TD	B2TD	B3TD	B4TD	Aquo-ion [27]
$^6H_{11/2}$	5922	5981	5981	5977	5992	5850
$^6F_{11/2}$	7837	7849	7843	7837	7837	7700
$^6F_{9/2}$	9158	9149	9166	9158	9149	9100
$^6F_{7/2}$	11,124	11,136	11,186	11,161	11,211	11,000
$^6F_{5/2}$	12,500	12,531	12,453	12,469	12,500	12,400
$^6F_{3/2}$	13,387	13,369	13,369	13,405	13,387	13,250
$^4F(3)_{9/2}$	21,231	21,186	21,142	21,231	21,277	21,100
$^4I(3)_{15/2}$	22,173	22,222	22,173	22,173	22,124	22,100
$^4G(4)_{11/2}$	23,585	23,585	23,585	–	23,640	23,400
$^4I(3)_{13/2}$	25,510	25,576	–	–	–	25,800
$\bar{\beta}$	1.007	1.009	1.010	1.011	1.012	
δ	−0.718	−0.871	−1.007	−1.079	−1.151	

Table 4
Experimental and calculated oscillator strengths ($\times 10^{-6}$) and Judd–Ofelt ($\times 10^{-20}$ cm^2) parameters of Dy^{3+} doped boro-tellurite glasses.

Transition	B0TD		B1TD		B2TD		B3TD		B4TD	
	f_{exp}	f_{cal}	f_{exp}	f_{cal}	f_{exp}	f_{cal}	f_{exp}	f_{cal}	f_{exp}	f_{cal}
$^6H_{11/2}$	1.083	1.140	1.100	1.161	0.921	1.269	0.956	1.182	0.773	0.916
$^6F_{11/2}$	6.524	6.519	7.965	7.957	8.381	8.337	8.168	8.139	7.313	7.294
$^6F_{9/2}$	1.884	1.879	1.893	1.888	1.684	1.877	1.580	1.705	1.340	1.386
$^6F_{7/2}$	1.617	1.674	1.468	1.533	2.433	1.654	1.983	1.482	1.201	1.060
$^6F_{5/2}$	1.116	0.808	1.065	0.706	0.852	0.785	0.757	0.699	0.822	0.468
$^6F_{3/2}$	0.098	0.153	0.142	0.133	0.132	0.149	0.115	0.133	0.120	0.089
$^4F(3)_{9/2}$	0.096	0.130	0.070	0.117	0.083	0.127	0.098	0.113	0.154	0.081
$^4I(3)_{15/2}$	0.324	0.392	0.312	0.386	0.366	0.422	0.318	0.393	0.085	0.297
$^4G(4)_{11/2}$	0.180	0.050	0.171	0.063	0.102	0.055	0.120	0.051	–	–
$^4I(3)_{13/2}$	0.983	0.199	0.737	0.204	–	–	–	–	–	–
N		10		10		9		9		8
σ		±0.272		±0.210		±0.294		±0.192		±0.165
Ω_2		7.553		9.100		9.575		8.045		9.229
Ω_4		1.252		1.548		1.258		1.196		1.147
Ω_6		1.918		1.636		1.778		1.022		1.556
Ω_4/Ω_6		0.653		0.946		0.708		1.170		0.737
Ref. index		1.596		1.624		1.656		1.682		1.704

lated oscillator strengths (f_{cal}) of an electric dipole transition from the ground state to excited state have been calculated using the following equation:

$$f_{cal} = \left[\frac{8\pi^2 mc\nu}{3h(2J+1)}\right]\left[\frac{(n^2+2)^2}{9n}\right] \times \sum_{\lambda=2,4,6} \Omega_\lambda (\Psi J \| U^\lambda \| \Psi' J')^2 \quad (4)$$

where ν is the wave number (cm^{-1}) of the transition from ground state (ΨJ) to excited state ($\Psi' J'$), n is the refractive index, c is the velocity of light in vacuum, m is the rest mass of an electron and $||U^\lambda||^2$ are the doubly reduced matrix elements evaluated in the intermediate coupling approximation for the state ΨJ to $\Psi' J'$ which are almost independent of the host matrix. The experimental oscillator strengths (f_{exp}) are calculated using Eq. (3) for observed transitions. The calculated oscillator strengths can be determined using Eq. (4). A least square fitting method is then used to determine the Ω_λ ($\lambda = 2$, 4 and 6) parameters which give the best fit between experimental and theoretical oscillator strengths. The experimental and calculated oscillator strengths for various transitions by taking all the observed levels (N) along with σ values and JO parameters for the prepared Dy^{3+}:BXTD glasses are presented in Table 4. The rms deviation of Dy^{3+}:BXTD glasses corresponding to B0TD, B1TD, B2TD, B3TD and B4TD glasses is ±0.273, ±0.210, ±0.294, ±0.192 and ±0.165 respectively. The values of the oscillator strengths in the present work are similar to those reported for other Dy^{3+} doped glasses [16,24,25].

The intense transitions lying between the $^6H_{15/2}$ ground state and the ^6H and ^6F terms in the infrared region are the spin allowed transitions ($\Delta S = 0$). The transitions within the ^6H term are allowed by the selection rule on the orbital angular momentum $\Delta L = 0$ and hence they are intense. The agreement between the experimental and calculated oscillator strengths is good for the intense transitions and moderate in the case of weak transitions. The spectral intensity of the hypersensitive transition ($^6F_{11/2}$) is found to be more than the other transitions.

It is observed from Table 4 that the value of JO parameter, Ω_2 is higher when compared to other two values Ω_4 and Ω_6 for all the glasses and follows the trend as $\Omega_2 > \Omega_6 > \Omega_4$. Jacob and Weber [26] reported that the Ω_4/Ω_6 ratio called as spectroscopic quality factor which is used to characterize the quality of the prepared glasses and based on the magnitude of spectroscopic quality factor (Ω_4/Ω_6) in the present work, Dy^{3+}:B3TD glass appears to be a better optical glass. The larger spectroscopic quality factor predict higher stimulated emission cross section among the prepared glasses. The JO parameters of the Dy^{3+}:BXTD glasses are found to be similar and comparable to other reported borate, boro-tellurite and fluorophosphate glasses [14,27,28]. Among the JO parameters Ω_2 is more sensitive to the local structure of the RE ion and inturn depends strongly on the hypersensitive transition and the higher value of Ω_2 is due to the relatively higher value of the oscillator strength of the hypersensitive transition. The JO parameters in general provide information about the nature of bond between RE ion and the surrounding ligands and also the symmetry of the environment around the RE ions. The variation of Ω_2 values within the BXTD glasses is in good agreement with the bonding parameter values.

3.4. Luminescence spectra and radiative properties

The luminescence spectra of the Dy^{3+}:BXTD glasses were recorded at room temperature in the wavelength range 450–750 nm by choosing the excitation wavelength as 375 nm and the same is presented in Fig. 4. The luminescence spectra exhibit three emission band peaks at 480 nm, 573 nm and 662 nm corresponding to $^4F_{9/2} \rightarrow {}^6H_{15/2}$ (blue), $^6H_{13/2}$ (yellow), $^6H_{11/2}$ (red) transitions respectively. The luminescence spectra of these glasses are similar to other reported Dy^{3+}:glasses [16,18,27]. The $^4F_{9/2} \rightarrow {}^6H_{13/2}$ transition is hypersensitive, and its intensity is

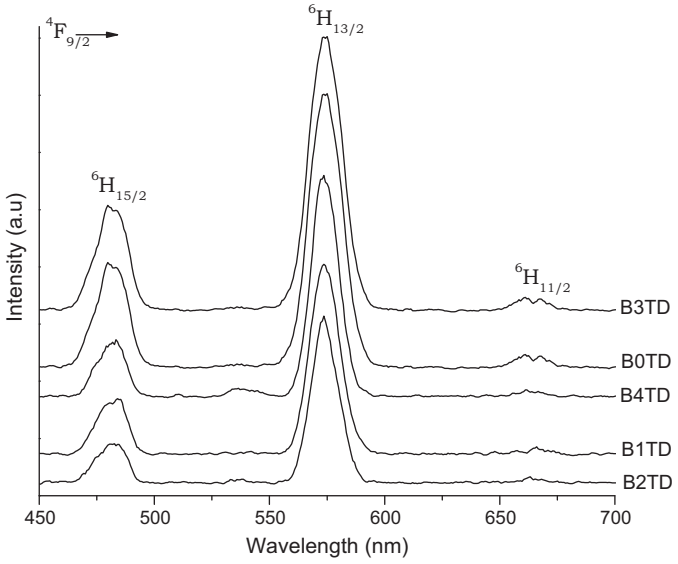

Fig. 4. Luminescence spectra of the Dy^{3+} boro-tellurite glasses.

Table 5
Emission band position (λ_p, nm), effective band width ($\Delta\lambda_{eff}$, nm), radiative transition probability(A, s^{-1}), peak stimulated emission cross section ($\sigma_P^E \times 10^{-22}$ cm^2), experimental and calculated branching ratios (β_R) for $^4F_{9/2}$ transition level of Dy^{3+}:boro-tellurite glasses.

Transition parameters	BOTD	B1TD	B2TD	B3TD	B4TD	
$^4F_{9/2} \rightarrow {}^6H_{15/2}$	λ_p	481.54	482.89	482.89	482.20	482.17
	$\Delta\lambda_{eff}$	10.31	9.40	9.40	9.88	9.67
	A	161.21	157.38	157.38	170.01	114.78
	σ_P^E	4.38	4.27	4.27	4.50	2.93
	β_R (exp)	0.259	0.204	0.204	0.208	0.219
	β_R (cal)	0.140	0.108	0.108	0.116	0.089
$^4F_{9/2} \rightarrow {}^6H_{13/2}$	λ_p	574.38	573.61	573.83	573.72	573.68
	$\Delta\lambda_{eff}$	8.49	7.96	7.26	7.00	7.23
	A	752.22	900.78	1003.28	1005.57	885.12
	σ_P^E	50.23	61.64	70.24	75.31	60.59
	β_R (exp)	0.710	0.736	0.763	0.761	0.751
	β_R (cal)	0.655	0.679	0.686	0.683	0.688
$^4F_{9/2} \rightarrow {}^6H_{11/2}$	λ_p	664.57	665.13	661.79	662.79	664.62
	$\Delta\lambda_{eff}$	6.58	6.69	6.49	5.84	4.60
	A	89.50	109.16	122.68	121.16	112.62
	σ_P^E	13.82	16.06	17.00	19.37	21.83
	β_R (exp)	0.032	0.043	0.033	0.031	0.030
	β_R (cal)	0.078	0.082	0.084	0.082	0.088

strongly influenced by the surrounding environment of Dy^{3+} ion, and the $^4F_{9/2} \rightarrow {}^6H_{11/2}$ transition is found to be weak in intensity. It is note worthy to observe that the ratio of $^4F_{9/2} \rightarrow {}^6H_{13/2}$ and $^4F_{9/2} \rightarrow {}^6H_{15/2}$ transitions (Y/B) values changes with the change in chemical composition.

The Y/B ratio is more sensitive to the glass composition and in the present work the Y/B ratio values are 2.744, 3.325, 3.664, 3.743 and 3.431 corresponding to Dy^{3+}:B0TD, B1TD, B2TD, B3TD and B4TD glasses respectively. The full width at half maximum (FWHM) of these blue and yellow emissions are 15.72 nm and 14.11 nm, respectively for the Dy^{3+}:B3TD glass. The luminescence intensity changes with the change in glass composition, and it is observed from the luminescence spectra that Dy^{3+}:B3TD glass exhibits strongest emission of all the studied glasses. No change in the shape or peak position of the broad emission could be observed. The observed line widths are large and it may be due to inhomogeneous local fields in the glass. The energy position of the $^4F_{9/2} \rightarrow {}^6H_{13/2}$ emission exhibits smaller variations (17,433–17,410 cm^{-1}), which implies that the interactions of the Dy^{3+} ions with the glass composition are almost similar irrespective of the change in chemical composition. An efficient laser transition has been characterized by a large stimulated emission cross section and in the present study Dy^{3+}:B3TD glass exhibits higher stimulated emission cross section value.

The radiative properties such as radiative transition probability (A), radiative lifetime (τ_{rad}), stimulated emission cross section (σ_P^E) and branching ratios (β_R) are calculated for the $^4F_{9/2} \rightarrow {}^6H_{15/2}$, $^6H_{13/2}$ and $^6H_{11/2}$ transitions and are presented in Table 5. It is observed from the table that the experimental branching ratio values are in agreement with the theoretically predicted values using the Judd–Ofelt theory. The experimental branching ratio value is found to be maximum for $^4F_{9/2} \rightarrow {}^6H_{13/2}$ transition for Dy^{3+}:BXTD glass. The branching ratio values follow the trend as $^4F_{9/2} \rightarrow {}^6H_{13/2} > {}^6H_{15/2} >$ and $^6H_{11/2}$ for all the prepared Dy^{3+}:BXTD glasses. The peak stimulated emission cross section (σ_P^E) values for the $^4F_{9/2} \rightarrow {}^6H_{13/2}$ transition for the Dy^{3+}:BXTD glasses have been determined using the expressions specified in the reported literature [27] and they are found to be 50.237, 61.640, 70.240, 75.310 and 60.599 respectively for the Dy^{3+}:B0TD, B1TD, B2TD, B3TD and B4TD glasses which are quite comparable to the reported values in the literature [15,29,30]. The peak stimulated emission cross section (σ_P^E) values and the branching ratio (β_R) values for the $^4F_{9/2} \rightarrow {}^6H_{13/2}$ transition posses higher values compared to other transitions of the Dy^{3+}:glasses which is suitable for laser action. Among the emission transitions $^4F_{9/2} \rightarrow {}^6H_J$ (J = 15/2, 13/2 and 11/2) the $^4F_{9/2} \rightarrow {}^6H_{13/2}$ band at 574 nm shows higher emission cross-section, which indicates that yellow emission is dominant. From the tabulated results it is concluded that $^4F_{9/2} \rightarrow {}^6H_{13/2}$ transition corresponding to Dy^{3+}:B3TD glass is favorable for laser action since it posses higher stimulated emission cross section and branching ratio values among the prepared glasses.

3.5. Decay curve analysis

The fluorescence decay curve of the $^4F_{9/2} \rightarrow {}^6H_{13/2}$ transition has been measured for the Dy^{3+}:B1TD glass and is shown in Fig. 5. The decay curves are almost single exponential for all the glasses and the lifetime calculation is straightforward. The near single exponential is either due to the fast decay of excited state Dy^{3+} ions or comparatively lesser effect of ligands on the Dy^{3+} ions. The effective decay time have been determined using the following expression [31]

$$\tau_{exp} = \tau_{eff} = \frac{\int tI(t)dt}{\int I(t)dt} \quad (5)$$

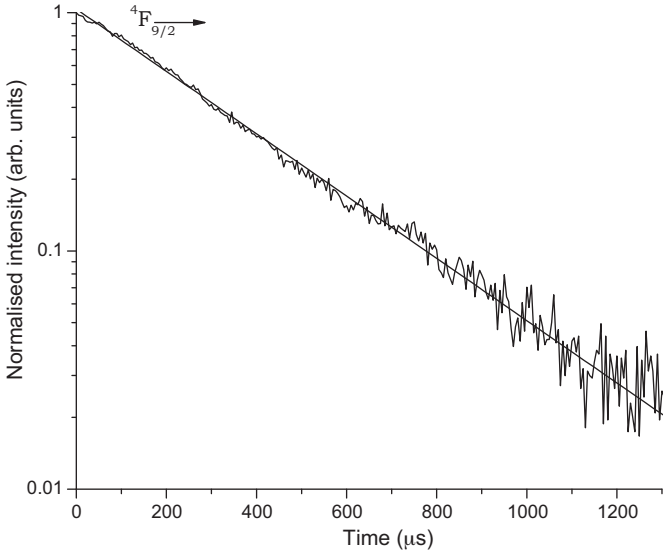

Fig. 5. Luminescence decay curve for $^4F_{9/2}$ state of Dy^{3+}:B1TD glass.

Table 6
Title of the glasses, energy (cm^{-1}), full width half maximum (nm), radiative and experimental lifetime (τ_{rad}, τ_{exp}, μs), Y/B ratio and quantum efficiency η (%) of the Dy^{3+}:BXTD glasses and other reported Dy^{3+} systems.

Sample code	$^4F_{9/2} \rightarrow {}_2\,{}^6H_{15/2}$ (blue)		$^4F_{9/22} \rightarrow {}_2\,{}^6H_{13/2}$ (yellow)		τ_{rad}	τ_{exp}	η (%)	Y/B
	Energy (cm^{-1})	FWHM (nm)	Energy (cm^{-1})	FWHM (nm)				
B0TD	20,767	16.93	17,410	16.13	870	593	68	2.744
B1TD	20,709	16.13	17,433	14.78	753	532	71	3.325
B2TD	20,738	16.80	17,430	12.77	679	478	70	3.664
B3TD	20,708	15.46	17,427	14.11	684	500	73	3.743
B4TD	20,739	15.72	17,431	13.11	778	480	62	3.431
Glass A [15]	20,747	–	17,452	–	876	596	68	–
Glass B [15]	20,790	–	17,452	–	954	612	64	–
Glass C [15]	20,747	–	17,422	–	607	580	95	–
Glass D [15]	20,790	–	17,391	–	642	567	88	–
Glass E [15]	20,747	–	17,422	–	853	600	70	–
Dy^{3+}:ZLB [17]	20,619	18	17,395	17	–	850	–	1.818
1BNLD [35]	20,790	–	17,422	–	428	405	95	0.875
3BNLD [35]	20,702	–	17,391	–	477	395	83	0.752
Lead borate [36]	20,833	18	17,452	14	638	447	70	1.08

where $I(t)$ is the emission intensity at time t. From the decay curves, lifetime (τ_{exp}) of the $^4F_{9/2}$ level has been determined by taking the first e-folding time of the decay intensity. Energy positions corresponding to the $^4F_{9/2} \rightarrow {}^6H_{13/2}$ transition and the experimental, calculated lifetime of the $^4F_{9/2}$ level of Dy^{3+} ions, quantum efficiencies along with other reported Dy^{3+} glasses are presented in Table 6. The energy position of the $^6H_{13/2}$ emission exhibits smaller variations (17,433–17,410 cm^{-1}), indicating the similar interactions of the Dy^{3+} ions irrespective of the change in chemical composition. The lifetime of the $^4F_{9/2}$ levels of Dy^{3+}:BXTD glasses is 593 μs, 532 μs, 478 μs, 500 μs and 480 μs respectively. The measured lifetime can be calculated from the equation [32]

$$\frac{1}{\tau_{exp}} = \frac{1}{\tau_{rad}} + W_{MPR} + W_{ET} \quad (6)$$

where τ_{rad} is the radiative lifetime calculated from JO theory. W_{MPR} is the multiphonon relaxation (MPR) and W_{ET} is the rate of energy transfer. The energy differences between the $^6F_{9/2}$ level and the next lower level are of about 6000 cm^{-1} which is large value, so the multiphonon relaxation negligible. It is observed from the table that, the experimental lifetime of $^4F_{9/2}$ level is found to be lower than the reported borate, phosphate and fluoro phosphate glasses [14,15,17]. The discrepancy between the τ_{exp} and τ_{rad} may be due to the non-radiative relaxation (W_{NR}) of excited Dy^{3+} ions.

The quantum efficiency (η) is defined as the ratio of the number of photons emitted to the number of photons absorbed. The quantum efficiency of the $^4F_{9/2}$ exited state is calculated using the following equation [33,34],

$$\eta = \frac{\tau_{exp}}{\tau_{rad}} \times 100\% \quad (7)$$

The η values are found to be 68, 71, 70, 73 and 62 respectively for the Dy^{3+}:B0TD, B1TD, B2TD, B3TD and B4TD glasses respectively.

4. Conclusion

The Dy^{3+} doped boro-tellurite glasses have been prepared and their structural and spectroscopic behavior were discussed and reported. The XRD pattern confirms the amorphous nature of the prepared glasses. The FTIR studies exhibit the B–O vibrations of BO_4 units in triborate, tetraborate and pentaborate groups associated with the prepared glasses. The presence of Te–O–Te linkage bending vibrations and the Te–O stretching mode of TeO_3 and TeO_6 units were explored when the tellurium dioxide content increases. The bonding parameters of the prepared glasses indicate the ionic nature. The *J–O* intensity parameters and the oscillator strengths were calculated from absorption spectra and discussed. Through the luminescence spectra, the peak wavelength, stimulated emission cross section and branching ratios were calculated for $^4F_{9/2} \rightarrow {}^6H_{15/2}$, $^6H_{13/2}$, $^6H_{11/2}$ transitions and the results were discussed and reported. The stimulated emission cross section for the Dy^{3+}:B3TD glass possess higher value and therefore it is suggested for suitable laser applications. It is observed from the luminescence spectra that the Y/B ratio values corresponding to $^4F_{9/2} \rightarrow {}^6H_{13/2}$ and $^4F_{9/2} \rightarrow {}^6H_{15/2}$ transitions change with the change in chemical composition and this could be used for suitable laser action. The decay curve of the $^4F_{9/2}$ level of Dy^{3+}:BXTD glasses is well fitted for single exponential and the quantum efficiency has been calculated and discussed.

References

[1] S. Suresh, M. Prasad, G. Upender, V. Kamalaker, V. Chandra Mouli, Indian J. Pure Appl. Phys. 47 (2009) 163–169.
[2] G.El. Dumrawi, Phys. Chem. Glasses 42 (2001) 56–60.
[3] Y. Gao, Q.-H. Nie, T.-F. Xu, X. Shen, Spectrochim. Acta Part A 61 (2005) 2822–2826.
[4] R.R. Reddy, Y. Nazeer Ahamed, P. Abdul Azeem, K. Rama Gopal, T.V.R. Rao, S. Buddhudu, N. Sooraj Hussin, J. Quant. Spectrosc. Radiat. Transfer 77 (2003) 149–163.
[5] H. Munemura, K. mitome, M. Misawa, K. Maruyama, J. Non-Cryst. Solids 200 (2001) 293–295.
[6] I. Ardelean, M. Peteanu, V. Simon, O. Cozar, F. Cioreas, S. Lapsor, J. Magn. Magn. Mater. 253 (1999) 196–197.
[7] J.S. Wang, E.M. Vogel, E. Snitzer, Opt. Mater. 3 (1994) 187–203.
[8] K. Marimuthu, S. Surendra Babu, G. Muralidharan, S. Arumugam, C.K. Jayasankar, Phys. Status Solidi A 206 (2009) 131–139.
[9] S. Rada, M. Culea, E. Culea, J. Non-Cryst. Solids 354 (2008) 5491–5495.
[10] S. Suresh, V. Chandra Mouli, Ferroelectrics 325 (2005) 105–109.
[11] R.T. Karunakaran, K. Marimuthu, S. Surendra Babu, S. Arumugam, Solid State Sci. 11 (2009) 1882–1889.
[12] L. Griguta, I. Ardelean, Mod. Phys. Lett. B 21 (2007) 1767–1774.
[13] R. Ciceo Lucacel, I. Ardelean, J. Optoelect. Adv. Mater. 8 (2006) 1124–1128.
[14] S. Surendra Babu, P. Babu, C.K. Jayasankar, Th. Troster, W. Sievers, G. Wortmann, Opt. Mater. 31 (2009) 624–631.
[15] P. Abdul Azeem, S. Balaji, R.R. Reddy, Spectrochem. Acta Part A 69 (2008) 183–188.
[16] C.K. Jayasankar, E. Rukmini, Physica B 240 (1997) 273–288.
[17] A. Thulasiramudu, S. Buddhudu, Spectrochim. Acta Part A 67 (2007) 802–807.
[18] R.T. Karunakaran, K. Marimuthu, S. Surendra Babu, S. Arumugam, J. Lumin. 130 (2010) 1067–1072.
[19] C.K. Jayasankar, P. Babu, J. Alloys Compd. 307 (2000) 82–95.
[20] A. Speghini, M. Peruffo, M. Casarin, D. Ajo, M. Bettinelli, J. Alloys Compd. 300 (2000) 174–179.
[21] W.T. Carnall, K.A. Gschneidner, L. Eyring (Eds.), Handbook on the Physics and Chemistry of Rare Earths, vol. 3, North-Holland, Amsterdam, 1987 (Chapter 24).
[22] B.R. Judd, Phys. Rev. 127 (1962) 750–761.
[23] G.S. Ofelt, J. Chem. Phys. 37 (1962) 511–521.
[24] Y.G. Choi, J. Heo, J. Non-Cryst. Solids 217 (1997) 199–207.
[25] A. Florez, V.A. Jerez, M. Florez, J. Alloys Compd. 303 (2000) 355–359.
[26] R.R. Jacobs, M.J. Weber, IEEE J. Quantum Electron. 12 (1976) 102–111.
[27] P. Babu, C.K. Jayasankar, Opt. Mater. 15 (2000) 65–79.

[28] K. Binnemans, R. Van Deun, C. Gorller-Walrand, J.L. Adam, J. Non-Cryst. Solids 238 (1998) 11–29.
[29] V.M. Orera, P.J. Alonso, R. Cases, R. Alcala, Phys. Chem. Glasses 29 (1988) 59–62.
[30] R. Praveena, R. Vijaya, C.K. Jayashankar, Spectrochim. Acta Part A 70 (2008) 577–586.
[31] G.C. Righini, M. Ferrari, Riv. Nuovo Cimento 28 (2005) 1–53.
[32] J. Sanz, R. Casess, R. Alcala, J. Non-Cryst. Solids 93 (1987) 377–386.
[33] C. Jacinto, S.L. Oliveira, L.A.O. Nunes, T. Catunda, M.J.V. Bell, J. Appl. Phys. 100 (2006) 113103.
[34] J. Pisarska, J. Phys. Condens. Matter 21 (2009) 285101.
[35] I. Arul Rayappan, K. Marimuthu, S. Surendra Babu, M. Sivaraman, J. Lumin. 130 (2010) 2407–2412.
[36] J. Pisarska, Opt. Mater. 31 (2009) 1784–1786.